Pergamon

Int. J. Multiphase Flow Vol. 20, No. 2, pp. 285–303, 1994

0301-9322/94 $7.00 + 0.00

THE PRESSURE LOSS AND SLUG FREQUENCY OF LIQUID–LIQUID–GAS SLUG FLOW IN HORIZONTAL PIPES

H. HERM STAPELBERG and D. MEWES
Institut für Verfahrenstechnik, University of Hannover, 30167 Hannover, Germany

(Received 4 October 1991; in revised form 30 August 1993)

Abstract—Experiments were performed which took into account the influence of a second immiscible liquid upon gas–liquid slug flow. Well-known models for the prediction of the slug frequency and pressure loss, as well as the flow pattern maps of two-phase flow, were extended for this special kind of multiphase flow.

Key Words: three-phase flow, liquid–liquid flow, slug flow, horizontal pipe, pressure loss, flow regimes

1. INTRODUCTION

The flow of two immiscible liquids (i.e. crude oil and water) and a gas is being encountered more and more in the offshore production of oil and gas. Although there is a large number of experimental and theoretical results on gas–liquid flow, known results for three-phase flow are small. In particular, the region of slug flow is of great interest in the offshore production of hydrocarbons.

Tek (1961) derived a procedure for calculating the pressure losses of three-phase flows. The method of calculation is simplified because he assumed averaged liquid properties for the two immiscible liquids. In this way, he reduced the three-phase flow to the problem of gas–liquid flow. Gregory & Fogarasi (1985) pointed out that averaged liquid properties cause large errors in theoretical predictions compared to experimental data.

Açikgöz *et al.* (1992) published experimental results for the establishing flow pattern of the three-phase flow. They considered similar flow regimes known from gas–liquid flow, but also took into account which phase was flowing dispersly or continuously. However, a prediction of the transition lines between the flow patterns for other liquid mixtures or pipe geometries is not yet possible. Açikgöz *et al.* (1992) as well as Lahey *et al.* (1992) derived drift–flux expressions for horizontal three-phase flows in order to predict the phase volumetric fractions for air–water–oil flows.

The aim of the investigation presented here is to show what difference it makes if one or two immiscible liquids flow in a horizontal pipe together with the gas, and how it is possible to extend frequently-used two-phase models to three-phase flow; the slug flow being the most important point of interest.

2. EXPERIMENTAL

In the experimental investigations on oil, water and air flow in horizontal pipes, two different diameters were used. The inside diameters of the investigated tubes were 23.8 and 59.0 mm.

The experimental facility is presented schematically in figure 1. Water and oil are supplied from separate storage vessels into the test pipe. Air is taken from a compressed air station. In order to enable the observation of the flow pattern, the whole pipeline is manufactured of acrylic glass. After passing through a 9.0 m long entrance section, the pressure loss is measured and the flow pattern observed. The mixing of the oil, water and air is achieved by an inlet nozzle. This nozzle is cone shaped and is separated into three sections by baffle plates. In this way the oil, water and air enter the pipeline stratified in layers according to their density. The exit diameter of the inlet nozzle equals the diameter of the pipeline attached to it. Due to this design, the water, oil and air are accelerated

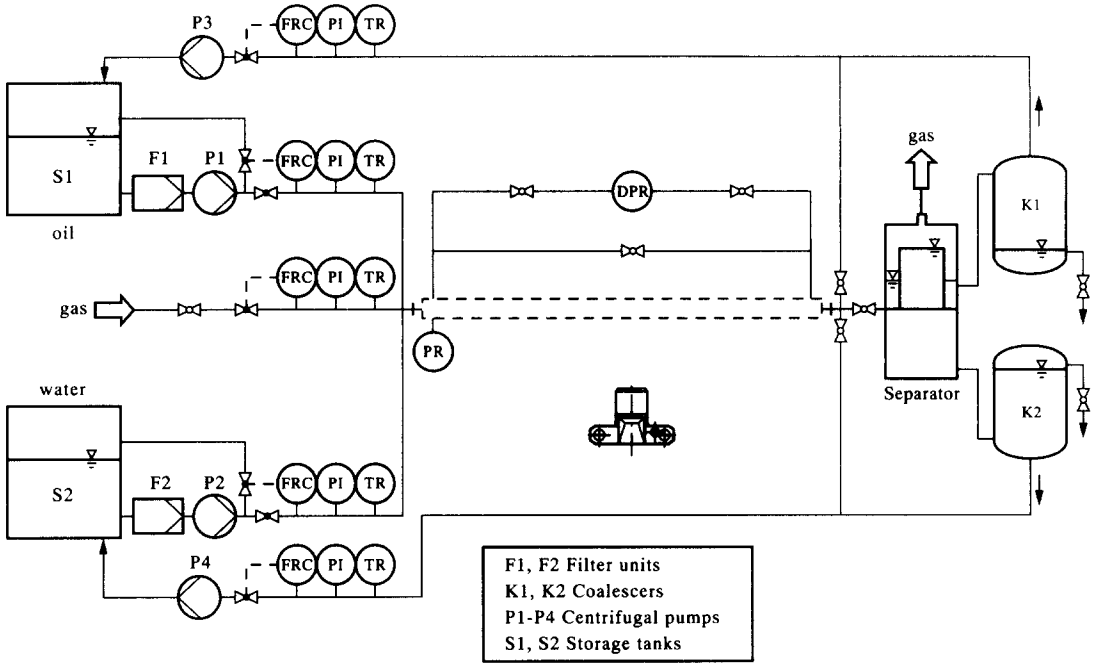

Figure 1. Experimental setup.

in the nozzle. For this reason the velocity profile is uniform at the entrance of the pipeline. Therefore, a fast development of the flow pattern in the test section is possible. The total length of the multiphase flow pipeline is 35 m.

In order to enable the recirculation of the liquids within the test facility, the outlet of the test section is connected to a separator unit, which separates the oil, water and gas. The preseparator is vented to the atmosphere. The oil and water are separated due to gravity. In order to separate the oil and water up to the limit of solubility, two coalescers are used for the small oil droplets in the water and vice versa. The cleaned fluids are pumped back into the storage vessels.

In two- and three-phase flows, the velocities of the slug front and the lengths and frequencies of the slugs observed must be measured. For the measurements of these parameters, it is necessary to determine the time the slug needs to pass a certain part of the test section. Therefore, this measurement is incorporated into the experimental setup. The beam of an He–Ne laser with a spectral output of 10 mW passes the test section tube horizontally at two locations. The light beam and the receiver photodiode are adjusted in such a way that the laser hits the photodiode directly in the case when air passes through the transilluminated part of the tube. When the light beam passes through the Plexiglas tube at its upper third portion, the situation is characteristic of film flow between two slugs. If the light path is traversed by the liquid phase, the light beam is refracted due to the change in the refractive index, and it can no longer reach the receiver photodiode.

In the experiments, in addition to air and water, a white mineral oil is used. The physical properties are determined for the conditions when the investigated liquid is saturated by the other one. Under ambient conditions 0.05 wt% water is soluble in oil and 0.5 wt% oil in water. The surface tension between the oil and water was measured using the droplet volume method, as described by Backes (1984). A comparison with the physical property values measured by Pfender (1986) shows good agreement. For ambient conditions, the density of the oil is 858 kg/m^3, the viscosity of oil is 31.0 mPa s and the surface tension between the oil and water is 53.5 mN/m.

3. THEORY FOR TWO-PHASE FLOW

3.1. Flow of Two Immiscible Liquids

Experimental results on the flow of two immiscible liquids serve as the limiting conditions for the interpretation of the results on the three-phase flow of water, oil and air. Known equations

for the calculation of the frictional pressure loss correspond either to a specific flow pattern or are based on the assumption that the oil and water flow under no-slip conditions. In the following section empirical correlations are given for the measured frictional pressure loss, which can be applied without knowledge of the particular flow pattern present in a specific case.

3.1.1. Flow patterns

In the flow of two immiscible liquids, different phase distributions have been observed in the flow cross section and along the flow path.

The first general presentation of the flow patterns was given by Guzhov *et al.* (1973). The immiscible liquids used were transformer oil and water. The flow pattern map is presented in figure 2. In the diagram, the total volumetric flux of both phases,

$$w_f \equiv \frac{1}{F}(\dot{V}_{f2} + \dot{V}_{f1}), \qquad [1]$$

is presented as function of the volume flow fraction of the water phase;

$$\dot{\varepsilon}_{f1} \equiv \frac{\dot{V}_{f1}}{\dot{V}_{f1} + \dot{V}_{f2}}. \qquad [2]$$

The volume flow rate is denoted by $\dot{V}$ and F is the cross-sectional area of the tube. The subscript f1 refers to the water and f2 to the oil. In the region of low volume flow rates, the phases form layers in the tube corresponding to their density differences. Only for high fractions of water flow is the oil phase distributed in the form of droplets, although a clear water layer can still be distinguished. For higher volume flow rates, the reverse phenomenon can be observed: water droplets moving beneath a clear oil layer. At even higher volume flow rates, a complete dispersion of the water phase is observed and a direct transition of the flow pattern from water droplet flow into oil droplet flow occurs. Below this volume flow rate, transitional regions can be recognized.

Arirachakaran *et al.* (1989) selected the same diagram for their flow pattern map as Guzhov *et al.* (1973). They varied the viscosities of the liquids over a wide range and observed annular flow as an additional flow pattern. One phase flows in the core of the tube and is surrounded by the other phase. The corresponding flow pattern map is presented in figure 3.

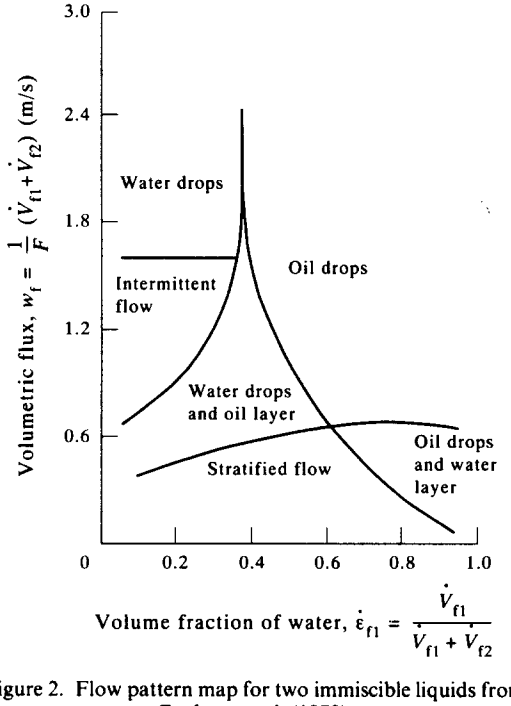

Figure 2. Flow pattern map for two immiscible liquids from Guzhov *et al.* (1973).

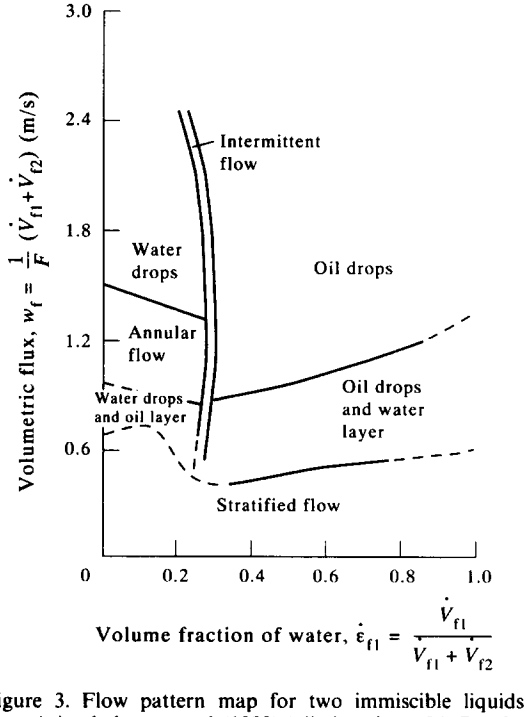

Figure 3. Flow pattern map for two immiscible liquids from Arirachakaran *et al.* (1989) (oil viscosity = 84 cP, tube diameter = 38.1 mm).

Further experimental results of the flow of two immiscible liquids are given by Herm Stapelberg (1991) and Brauner (1991). These, however, are predominantly limited to stratified flow or annular flow, so a generalization of these results is not possible.

3.1.2. Calculation of the frictional pressure loss

Besides the flow pattern map for oil and water, Arirachakaran *et al.* (1989) presented a method for calculating the frictional pressure loss in these flows. They assume a homogeneous flow of oil and water and distinguish between stratified flow and droplet flow patterns.

The volume flow fraction of the oil is

$$\dot{\varepsilon}_{f2} \equiv \frac{\dot{V}_{f2}}{\dot{V}_{f2} + \dot{V}_{f1}}. \qquad [3]$$

Without slip, homogeneous flow is present and the condition $\dot{\varepsilon}_{f2} = \varepsilon_{f2}$ applies, where the volume fraction of the oil phase is

$$\varepsilon_{f2} = \frac{V_{f2}}{V_{f2} + V_{f1}}. \qquad [4]$$

In [4] V_{f1} and V_{f2} are the volumes of the water phase (f1) and the oil phase (f2) inside the tube section, respectively. The average density and viscosity of the homogeneous mixture is—according to the proposed procedure—calculated by using the appropriate volume flow fractions:

$$\bar{\varrho} = \dot{\varepsilon}_{f2}\varrho_{f2} + (1 - \dot{\varepsilon}_{f2})\varrho_{f1} \qquad [5a]$$

and

$$\bar{\eta} = \dot{\varepsilon}_{f2}\eta_{f2} + (1 - \dot{\varepsilon}_{f2})\eta_{f1}. \qquad [5b]$$

The velocity total volumetric flux—the so-called superficial velocity—of the liquid two-phase mixture is

$$w_f = \frac{1}{F}(\dot{V}_{f2} + \dot{V}_{f1}). \qquad [6]$$

The pressure loss of the two-phase flow is

$$\left(\frac{\Delta p}{l}\right)_2 = \Psi_2 \frac{1}{d}\frac{\bar{\varrho} w_f^2}{2}. \qquad [7]$$

The drag coefficient Ψ_2 can be determined by known equations from single-phase flow using the fluid properties $\bar{\varrho}$ and $\bar{\eta}$, respectively.

Equations [5]–[7] are valid for droplet flow, as long as the phase inversion point (see figure 3) has not been achieved. The viscosity increases if phase separation occurs. A limiting value of the volume flow fraction of the oil phase $\dot{\varepsilon}_{f2,gr}$ can be given, for which phase inversion has to be considered:

$$\dot{\varepsilon}_{f2,gr} = 0.5 + 0.1108 \log(10^3 \eta_{f2}). \qquad [8]$$

The viscosity of the oil η_{f2} has to be entered in Pa s. If the oil and water are passing through the tube in layers stacked according to their density, the frictional pressure loss is calculated by another method (Arirachakaran *et al.* 1989). If the interface between the oil and water is smooth and there is no relative velocity between the phases, the pressure loss is given by the sum of the wall shear stresses for the tube wall wetted by the water and by the oil. The average wall shear stress is

$$\tau = \frac{s_{f2}}{s}\tau_{f2} + \frac{s_{f1}}{s}\tau_{f1}. \qquad [9]$$

In this equation s is the perimeter of the tube, s_{f2} is the section of the perimeter wetted by the oil and s_{f1} is the section wetted by the water. The relative velocity between the phases is neglected ($\dot{\varepsilon}_{f2} = \varepsilon_{f2}$) and

$$\frac{s_{f1}}{s} = \frac{\alpha}{2\pi} \quad \text{and} \quad \frac{s_{f2}}{s} = 1 - \frac{\alpha}{2\pi}. \qquad [10]$$

The angle α can be calculated iteratively from the given cross section of the tube if the oil hold-up is known:

$$2\pi(1-\dot{\varepsilon}_{f2}) = \alpha - \sin\alpha. \qquad [11]$$

Further, it is assumed that the wall shear stress τ_{f1} and τ_{f2} can be evaluated using the single-phase flow laws. For determining τ_{f2}, it is assumed that the total volume flow rate $(\dot{V}_{f2}+\dot{V}_{f1})$ passing through the tube is that of the oil; and for determining τ_{f1}, the total volume flow rate is that of the water. The frictional pressure loss of the two-phase flow is

$$\left(\frac{\Delta p}{l}\right)_2 = \frac{s_{f2}}{s}\left(\frac{\Delta p}{l}\right)_{m,f2} + \frac{s_{f1}}{s}\left(\frac{\Delta p}{l}\right)_{m,f1}; \qquad [12]$$

$(\Delta p/l)_m$ is the pressure loss in single-phase flow,

$$\left(\frac{\Delta p}{l}\right)_{m,f2} = \Psi_{f2}\frac{1}{d}\frac{\varrho_{f2}w_f^2}{2} \quad \text{or} \quad \left(\frac{\Delta p}{l}\right)_{m,f1} = \Psi_{f1}\frac{1}{d}\frac{\varrho_{f1}w_f^2}{2}. \qquad [13]$$

The Reynolds numbers needed for the calculation of the friction factors Ψ_{f2} and Ψ_{f1} are defined by the total volume flux w_f and the diameter d of the pipe:

$$\mathrm{Re}_{f2} = \frac{w_f d}{\nu_{f2}} \quad \text{and} \quad \mathrm{Re}_{f1} = \frac{w_f d}{\nu_{f1}}. \qquad [14]$$

The transition from laminar to turbulent flow is taken, in accordance with the value for single-phase flow, as 2300.

Following the recommendation of Charles & Lilleleht (1966) in figure 4, the pressure losses are presented in a Lockhart–Martinelli diagram. The pressure loss ratio

$$\Phi_{f2}^2 = \frac{\left(\frac{\Delta p}{l}\right)_2}{\left(\frac{\Delta p}{l}\right)_{f2}} \qquad [15]$$

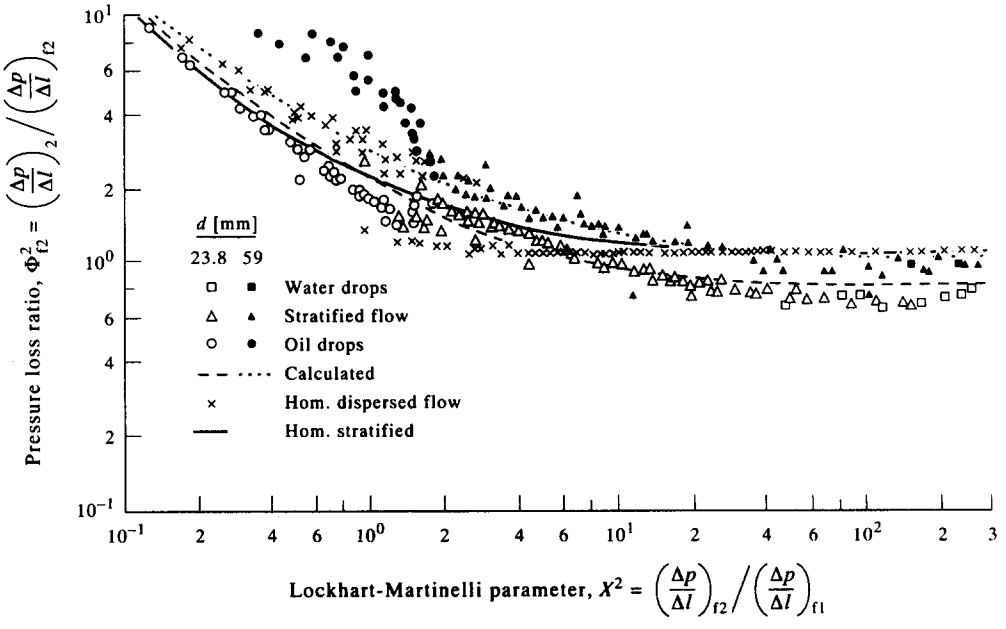

Figure 4. Lockhart–Martinelli diagram for the flow of two immiscible liquids.

is presented as a function of the Lockhard–Martinelli parameter

$$X^2 = \frac{\left(\frac{\Delta p}{l}\right)_{f2}}{\left(\frac{\Delta p}{l}\right)_{f1}}. \qquad [16]$$

The subscript 2 denotes the pressure loss when the oil and water flow together through the tube, and the subscript f denotes the pressure loss that would exist if pure oil (index f2) or pure water (index f1) were to flow through the pipe at the volume flow rate of each phase under consideration.

If the flow patterns can be determined correctly using the flow pattern map described previously then the friction pressure loss can be calculated according to the procedure given by Arirachakaran *et al.* (1989). The limiting laws of single-phase flow can be reproduced correctly—similarly to the homogeneous models. From these relationships, the asymptotic limits for the calculations are formed.

In figure 4, the frictional pressure losses calculated by [13]–[16] are compared with experimental results. Only for stratified flow can a continuous curve be drawn. In all other cases, both volume flow rates influence the calculated transition from laminar to turbulent flow. In particular, in the region of stratified flow the calculation procedure of Arirachakaran *et al.* (1989) is not applicable. In this region, pressure loss ratios were measured which give $\Phi_{f2}^2 < 1$. This is due to the pressure loss reduction caused by the addition of water, as mentioned by Charles (1960). In these regions the definition of the homogeneous model is not applicable. Similarly, no satisfactory agreement between the measured and calculated results can be achieved in the region of droplet flow using a homogeneous model for dispersed flow. The measured frictional pressure loss in this region is lower than the calculated one.

In order to recognize this behaviour and to enable the calculation of the frictional pressure loss independently of the particular flow pattern present in the investigated flow, the measured values are represented empirically using a heterogeneous model, analogous to that of Lockhart & Martinelli (1949) for gas–liquid flows. The whole range of laminar–laminar and laminar–turbulent oil–water flow is taken into account. Accordingly, the pressure loss ratio is finally only a function of the Lockhart–Martinelli parameter:

$$\Phi_{f2}^2 = f(X^2). \qquad [17]$$

For determining the pressure loss ratio Φ_{f2}^2, the correlation

$$\Phi_{f2}^2 = \frac{X^{i+1} + X^i + a}{X^{i+1} + aX} \qquad [18]$$

is selected, which gives results below $\Phi_{f2}^2 = 1$. By determining the parameters i and a using the minimization of the mean-square deviation technique, the exponent i in [18] is

$$i = 0.5589. \qquad [19]$$

The value of a depends on the tube diameter:

$$\left.\begin{aligned} a &= 1.10 \quad \text{for} \quad d = 23.8\ \text{mm} \\ \text{and} \\ a &= 0.46 \quad \text{for} \quad d = 59.0\ \text{mm}. \end{aligned}\right\} \qquad [20]$$

Equation [18] is shown in figure 4. Apart from the correct reproduction of the limiting laws for $X^2 \to 0$ and $X^2 \to \infty$, values of $\Phi_{f2}^2 < 1$ are obtained. The mean deviation for both investigated tube diameters is approximately 15%. In this way, an improved calculation procedure for the frictional pressure loss for oil–water flow is possible, compared to the results of the homogeneous model equation. However, the pressure losses in the oil drop region are not fitted so well by the chosen calculation procedure.

3.2. *Slug Flow of Gas and One Liquid*

Comprehensive procedures for the calculation of the pressure loss of two-phase slug flow were first developed by Dukler & Hubbard (1975) and later in an improved form by Aziz *et al.* (1978). In order to calculate the pressure loss, it is necessary to know the physical properties, the volume flow rates of the gas and liquid, the dimensions of the tube (see figure 5), the volume fraction of the gas in the slug body and the frequency of slug appearance. The volume fraction of the gas within the body of the slug is calculated, according to Aziz *et al.* (1978), by

$$\varepsilon_S = 1 - \left[1 + \left(\frac{w_f + w_G}{k_1}\right)^{k_2}\right]^{-1}. \qquad [21]$$

The coefficients are obtained as $k_1 = 8.66$ m/s and $k_2 = 1.39$, and match the experiments by Aziz *et al.* (1978).

3.2.1. *Slug frequency*

The first comprehensive experimental investigations on slug frequencies were performed by Hubbard (1965), who investigated the flow of air and water in a horizontal pipe with 35.1 mm i.d. The greater the superficial velocity of the water, the higher is the frequency of the liquid slugs flowing through the pipe. The measured slug frequencies have a minimum as a function of the volumetric flux of the gas phase. These observations were confirmed by the experimental investigations of Gregory & Scott (1969) and Taitel & Dukler (1977). Gregory & Scott (1969) observed this minimum for the situation when the sum of the volumetric fluxes of the gas and liquid is approximately 4.4 m/s. Gregory & Scott (1969) investigated the flow of carbon dioxide and air.

Tronconi (1990) adopted the recommendation of Taitel & Dukler (1977) and considered the slug frequency, because of slug formation from a wavy stratified flow. Apart from this, Tronconi assumed, according to Mishima & Ishii (1980), that the waves on a liquid surface would grow according to the Kelvin–Helmholtz instabilities, but only waves characterized by a critical growth rate cause the formation of a stable liquid slug. Thus, Tronconi postulated that a linear correlation holds between the frequency of the formation of critical waves and the slug frequency,

$$f_w = C_w f_S, \qquad [22]$$

and determined the value of the proportionality factor as $C_w = 2$. This means that from every second critical wave a stable slug is formed, which corresponds to the observations of slug flow by Dukler *et al.* (1985). Kordyban (1985) observed that 50% of the slugs originating from the critical wave are temporally instable and disappear. By using the proportionality factor C_w, Tronconi (1990) adopted the theory of Mishima & Ishii (1980) and obtained the slug frequency:

$$f_S = 0.305 C_w^{-1} \frac{\varrho_G}{\varrho_f} \frac{\bar{w}_G}{h_G}. \qquad [23]$$

In [23], h_G is the height of the gas-phase layer in the stratified flow, and $\bar{w}_G$ is the average gas velocity within the gas layer cross section of the pipe. According to Taitel & Dukler (1976), the liquid height is

$$h_f = d - h_G. \qquad [24]$$

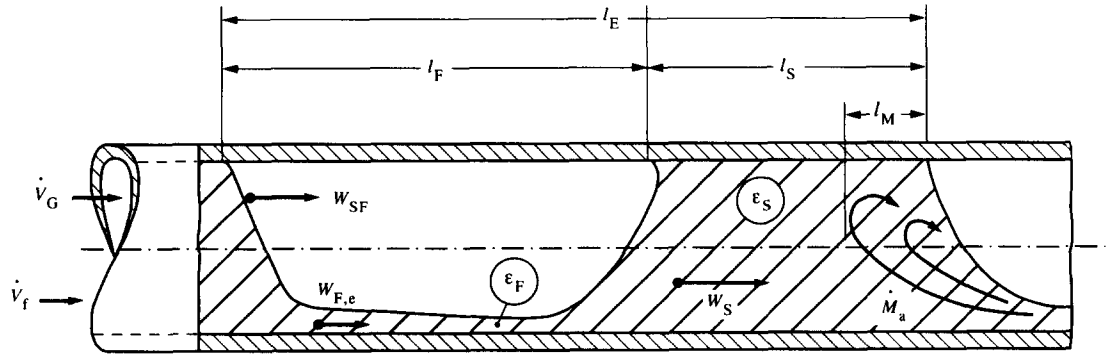

Figure 5. Simplified slug model.

The liquid height depends on the Lockhard–Martinelli parameter

$$X^2 = \frac{\left(\frac{\Delta p}{l}\right)_f}{\left(\frac{\Delta p}{l}\right)_G}, \qquad [25]$$

which can be calculated from the momentum balance equation:

$$X^2 = \frac{\left[\frac{s_G^*}{F_G^*} + \left(\frac{s_i^*}{F_f^*} + \frac{s_i^*}{F_G^*}\right)\frac{\Psi_f}{\Psi_G}\right]}{\frac{(w_f^* d_{h,f}^*)^{-n}}{(w_G^* d_{h,G}^*)^{-m}}\left(\frac{s_f^*}{F_f^*}\right)}\left(\frac{w_G^*}{w_f^*}\right)^2. \qquad [26]$$

All parameters on the right-hand side of [26] can be calculated as functions of the liquid height. In [26], s_f denotes the perimeter of the tube wetted by the liquid and s_G is the perimeter wetted by the gas. The length of the interface between the gas and the liquid is s_i. The non-dimensional parameters used in [26] are explained in table 1.

As a significant simplification of the selected evaluation procedure, Taitel & Dukler (1976) took the flow friction factors Ψ_f and Ψ_G of the liquid and gas phases to be equal:

$$\Psi_f = \Psi_G. \qquad [27]$$

This is in agreement with the experimental results from Gazley (1949) for smooth stratified flow. Tronconi (1990), however, stated that especially in the region of slug formation, the interface is wavy, therefore the friction factors should increase for increasing gas velocities. Tronconi therefore calculated the friction factor as a function of the Reynolds number of the gas flow (table 2). In this way, the height of the liquid or the gas layer can be calculated and the slug frequency can be determined.

A comparison of the measured slug frequencies given by Hubbard (1965), Gregory & Scott (1969), Kvernvold *et al.* (1984), Heywood & Richardson (1979), Vermeulen & Ryan (1971) and Kago *et al.* (1987) with the values calculated by [23] gives a mean deviation of $<17\%$. Only the measurements of Vermeulen & Ryan (1971) deviate by 50%. Tronconi (1990) stated that the tube

Table 1. Explanation of the dimensionless parameters in [26]

$$h_G = d - h_f \qquad [24]$$

$$h_f = f(X); \quad X^2 = \frac{\left(\frac{\Delta p}{l}\right)_f}{\left(\frac{\Delta p}{l}\right)_G}$$

$$X^2 = \frac{\left[\frac{s_G^*}{F_G^*} + \left(\frac{s_i^*}{F_f^*} + \frac{s_i^*}{F_G^*}\right)\frac{\Psi_f}{\Psi_G}\right]}{\frac{(w_f^* d_{h,f}^*)^{-n}}{(w_G^* d_{h,G}^*)^{-m}}\left(\frac{s_f^*}{F_f^*}\right)}\left(\frac{w_G^*}{w_f^*}\right)^2 \qquad [26]$$

$$\Psi_f = C_f = \left(\frac{\bar{w}_f d_{h,f}}{\nu_f}\right)^{-n} = C_f \mathrm{Re}_f^{-n}; \; d_{h,f} = \frac{4F_f}{s_f}$$

$$\Psi_G = C_G\left(\frac{\bar{w}_G d_{h,G}}{\nu_G}\right)^{-m} = C_G \mathrm{Re}_G^{-m}; \; d_{h,G} = \frac{4F_G}{s_f + s_G}$$

$$C_G = 0.046; \quad C_f = 16; \quad n = 1; \quad m = 0.2;$$

$h^* \equiv h_f/d$
$F_f^* \equiv 0.25\{\pi - \arccos(2h^* - 1) + (2h^* - 1)[1 - (2h^* - 1)^2]^{0.5}\}$,
$F_G^* \equiv 0.25\{\arccos(2h^* - 1) - (2h^* - 1)[1 - (2h^* - 1)^2]^{0.5}\}$,
$s_f^* \equiv \pi - \arccos(2h^* - 1)$; $F^* \equiv F/d^2 = \pi/4$,
$s_G^* \equiv \arccos(2h^* - 1)$; $F_f^* \equiv F_f/F$,
$s_i^* \equiv [1 - (2h^* - 1)^2]^{0.5}$; $F_G^* \equiv F_G/F$,
$w_f^* \equiv F^*/F_f^*$; $d_{h,f}^* \equiv d_{h,f}/d$,
$w_G^* \equiv F^*/F_G^*$; $d_{h,G}^* \equiv d_{h,G}/d$.

Table 2. Prediction of the friction factor at the tube wall Ψ_G and at the interface Ψ_f, from Tronconi (1990)

Re_G	Ψ_G	$\frac{\Psi_f}{\Psi_G}$
$\mathrm{Re}_G \leqslant 2500$	$16\,\mathrm{Re}_G^{-1}$	1
$2500 < \mathrm{Re}_G \leqslant 8000$	$1.98 \cdot 10^{-3}\,\mathrm{Re}_G^{0.15}$	$9.124 \cdot 10^{-3}\,\mathrm{Re}_G^{0.6}$
$\mathrm{Re}_G > 8000$	$0.046\,\mathrm{Re}_G^{-0.2}$	2

$$\mathrm{Re}_G = \frac{\bar{w}_G d_{h,G}}{\nu_G}; \quad \bar{w}_G = \frac{\dot{V}_G}{\varepsilon_G F}; \quad d_{h,G} = \frac{4F_G}{s_i + s_G}.$$

diameter of 12.7 mm used in the measurements was extremely small. Therefore, the surface tension can no longer be neglected, due to the curvature of the liquid surface in these pipes.

Our own experiments with water and air are in agreement with the values calculated by the method used by Tronconi (1990). In figure 6, the slug frequencies measured by the authors are compared with those calculated by [23]. Starting from low volumetric fluxes, the calculated slug frequencies are high and decrease with increasing volumetric fluxes. The measured slug frequencies increase with increasing volumetric fluxes. It has to be noted, that the procedures of Greskovich & Shrier (1972) and Tronconi (1990) are based on measurements with higher volumetric fluxes than the maximal values used in our experiments, where plug flow develops first. The plug bubbles first appear with high frequencies in the pipeline. With increasing volumetric fluxes of the gas phase, the plug bubbles join to form larger bubbles, and slug flow develops. The frequency decreases continuously with the change in the flow pattern. On the other hand, in the experimental investigations it was observed that slug flow developed directly from the stratified flow, which is characterized by a gradual increase in the slug frequency. Beyond a total volumetric flux of approximately 2 m/s, the measured and calculated values show a rather good agreement. Using [23] for volumetric fluxes > 2 m/s, higher values of slug frequencies were obtained with increasing velocity, which reproduce the measured results even better. Above these volumetric fluxes the mean deviation between the experiment and the values calculated by [23] is about $\pm 30\%$. It increases to $\pm 50\%$ when the method of Greskovich & Shrier (1972) is used.

A comparison of the measured and calculated slug frequencies is given in figure 7 for the flow of oil and air. Greskovich & Shrier (1972) only consider the volume flow rates of the phases and the tube diameter in their calculation procedure. The viscosity of the liquid is not considered. Therefore, the calculated slug frequencies are too low.

Conversely, Tronconi (1990) also considered the viscosity of the liquid. With increasing liquid viscosity, the height of the liquid in stratified flow and thus the volumetric flux of the gas phase increase (see [26]). Both these effects cause an increase in the calculated slug frequency, when the viscosity of the liquid increases under the assumption of constant volume flow rates. Regarding [23], it must be realized in the experiments described in this paper liquids of higher viscosity were used that only form a critical wave every third or fourth wave. The value of the factor C_w used

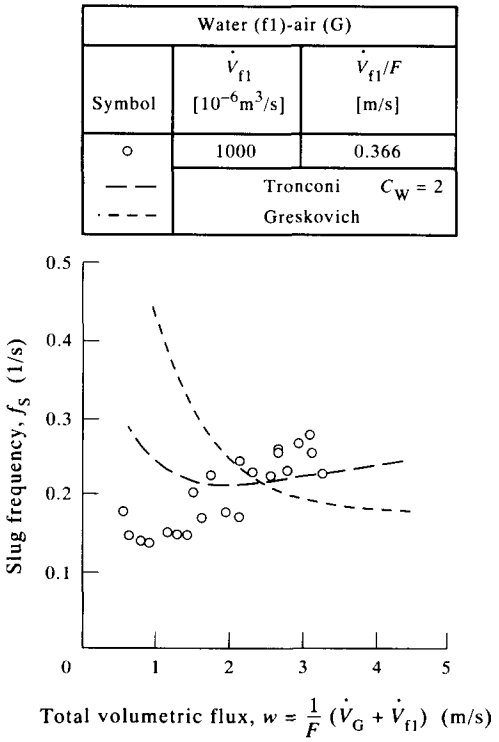

Figure 6. Comparison of the measured and predicted slug frequencies for the flow of air and water.

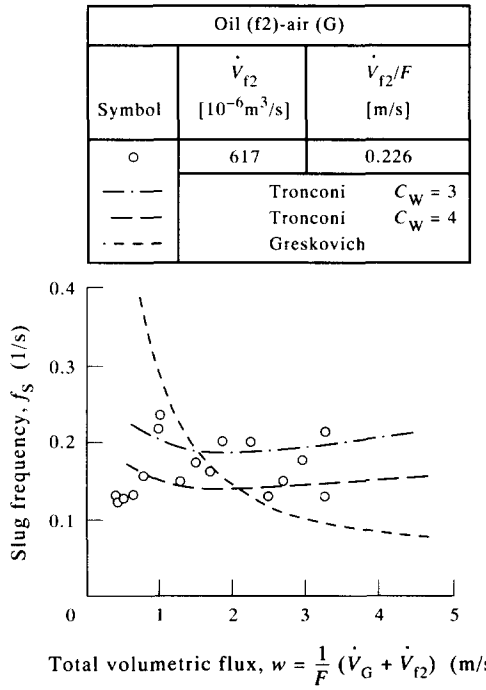

Figure 7. Comparison of the measured and predicted slug frequencies for the flow of air and oil.

in [23] is from our own experiments 3 or 4. The results of the calculations are given in figure 7. An agreement of the results can be found, similarly to the flow of water and air, only in the case when the sum of the volumetric fluxes exceeds 2.0 m/s. The mean deviation between the calculations and measurements is $\pm 22\%$, when C_w is taken to be 4. The measured frequencies fluctuate between the calculated ones according to the coefficients $C_w = 3$ and 4.

3.2.2. Calculation of the pressure loss in two-phase slug flow

The measured frictional pressure losses are compared with calculated values obtained using the correlations of Dukler & Hubbard (1975) and Aziz *et al.* (1978). As the agreement between the measured and calculated slug lengths has only been achieved within limited regions of the varied parameters, the slug frequency and the gas hold-up in the slug body are selected as additional necessary parameters in the calculation. According to the observations and comparisons discussed above, for the calculation of the gas hold-up in the slug body, the correlation of Aziz *et al.* (1978) is used, and for the calculation of the slug frequency [23] is used. The values of the coefficient were chosen to be $C_w = 2$ for the flow of water and air and $C_w = 3$ to 4 for the flow of oil and air.

In figure 8, measured and calculated frictional pressure losses are presented for the flow of water and air; and in figure 9, those for the flow of oil and air. The basic difference in the calculation procedures is the fact that Aziz *et al.* (1978) consider the total slug length in their calculations of the frictional pressure loss, whereas Dukler & Hubbard (1975) limit the frictional pressure loss to the length of the core region of the slug. The accelerational pressure losses in both calculation procedures are limited to the mixing region. Hence, lower values of the pressure losses are usually obtained by using the procedure of Dukler & Hubbard than by using the procedure of Aziz *et al.*

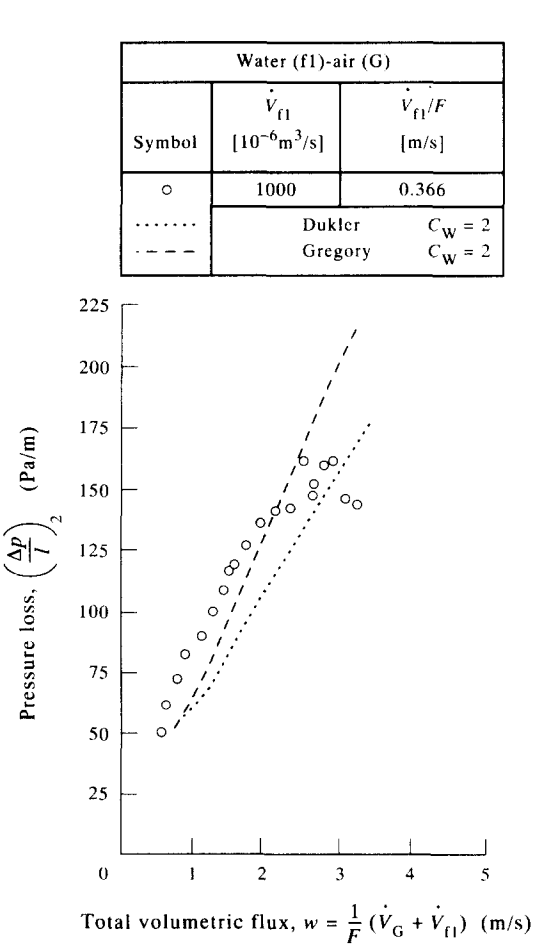

Figure 8. Comparison of the measured and predicted pressure losses for slug flow of air and water.

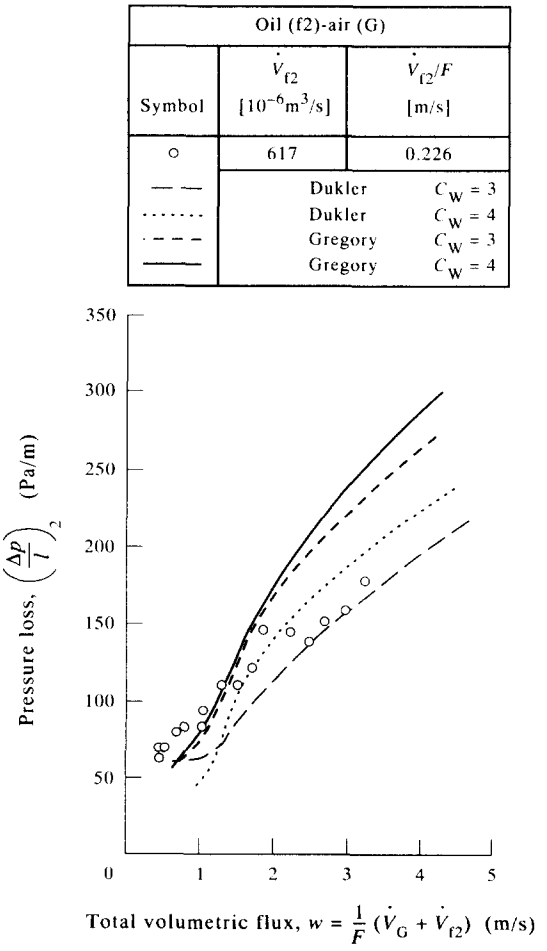

Figure 9. Comparison of the measured and predicted pressure losses for slug flow of air and oil.

The measured and calculated pressure losses for the flow of water and air deviate by $<32\%$, excluding the situation with very low volumetric fluxes of the gas phase in the transition region between stratified flow and slug flow. The mean deviations between all the measured values and the calculated values of Dukler & Hubbard (1975) are around 16%, and those between the values calculated by Aziz *et al.* (1978) are around 12%. Thus, it is possible to evaluate the pressure loss for water and air flow in the slug flow region with higher accuracy than it is to evaluate the pressure loss with the known homogeneous or heterogeneous models. By evaluating the slug frequency of the oil and air flow using the method of Tronconi (1990), the mean deviation compared to the results of Dukler & Hubbard (1975) is $\pm 17\%$.

4. THREE-PHASE FLOW OF WATER, OIL AND AIR IN HORIZONTAL TUBES

4.1. Observed Flow Patterns and the Flow Pattern Map

In horizontal three-phase oil–water–air flow, the same flow patterns are observed as in two-phase flow of a gas and a liquid, as long as the degree of dispersion of the oil and water is not taken into account. At low volume flow rates, the water, oil and air flow in layers corresponding to their density in the pipeline. With increasing volume flow rates, waves of low amplitude are first observed at the interface between the oil and water and subsequently also at the interface between the oil and air. Still, before the two immiscible liquids disperse from the wavy surface between the oil and water, the slug flow develops. In both tube diameters, the liquids continue to flow stratified in the slug flow regime—both in the slug body as well as in the film flow region between the slugs. In addition to this, an accumulation of water in the slug body can be recognized. If the slug velocity continues to increase due to the increase in the volume flow rate, then the immiscible liquids disperse into droplets, only partly at first and then completely. For the classification of the flow patterns, the level of dispersion of the oil and water is not taken into consideration. In figure 10, the flow pattern map for gas and liquid flow recommended by Baker (1954) is presented. The volume fraction of the oil is defined as follows:

$$\dot{\varepsilon}_{f2} = \frac{\dot{V}_{f2}}{\dot{V}_{f1} + \dot{V}_{f2}}; \qquad [28]$$

f1 denotes the water phase and f2 the oil phase. In figure 10, the transition lines between the different flow patterns are indicated, for the case when only water ($\dot{\varepsilon}_{f2} = 0$) or only oil ($\dot{\varepsilon}_{f2} = 1$) flows in the tube along with the air. The experiments with three-phase water–oil–air flow indicate that the transition lines between the observed flow patterns agree with those presented in the flow pattern map of figure 10, when the total volumetric flux of liquid phase is used. This is achieved by taking the average velocities $\bar{w}_{f1} \equiv \dot{V}_{f1}/(\varepsilon_{f1} F)$ and $\bar{w}_{f2} \equiv \dot{V}_{f2}/(\varepsilon_{f2} F)$. The superficial velocity of the homogeneous oil–water mixture is

$$w_f = (1 - \dot{\varepsilon}_{f2})\bar{w}_{f1} + \dot{\varepsilon}_{f2}\bar{w}_{f2}. \qquad [29]$$

For the three-phase flow, the transitional regions from stratified and wavy flow towards the intermittent flow are located between the lines for the two-phase gas–liquid flow presented in figure 10. If the transitional regions were to be calculated according to the extended flow pattern map of Baker for the three-phase flow situation, the density and the viscosity of the homogeneously flowing liquid has to be taken into consideration. It holds that

$$\bar{\varrho} = (1 - \dot{\varepsilon}_{f2}\varrho_{f1} + \dot{\varepsilon}_{f2}\varrho_{f2}) \qquad [30]$$

and

$$\bar{\eta} = (1 - \dot{\varepsilon}_{f2})\eta_{f1} + \dot{\varepsilon}_{f2}\eta_{f2}. \qquad [31]$$

The mass flow rate of the liquid is

$$\dot{m}_f = \frac{\bar{\varrho}(\dot{V}_{f1} + \dot{V}_{f2})}{F} = \bar{w}_{f1}\varrho_{f1} + \bar{w}_{f2}\varrho_{f2}. \qquad [32]$$

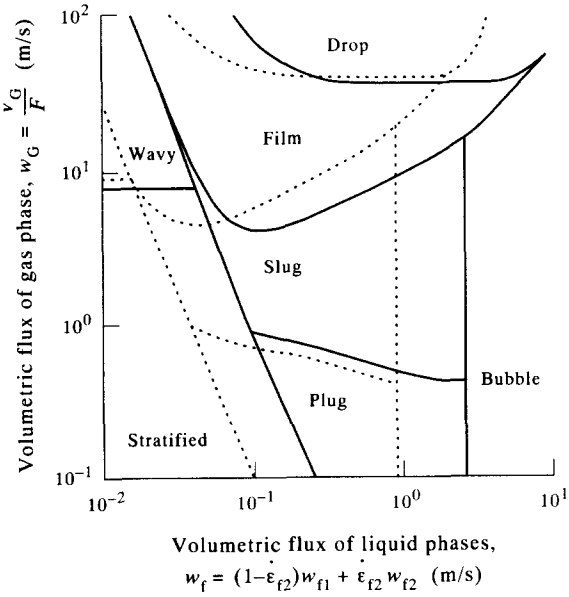

Figure 10. Baker's (1954) flow pattern map modified for three-phase flow.

Water (f1)-oil (f2)-air (G)			
	$\dot{V}_{f1} + \dot{V}_{f2}$	$\dot{V}_{f1} + \dot{V}_{f2}/F$	$\dot{V}_{f2} / (\dot{V}_{f1} + \dot{V}_{f2})$
Symbol	[10^{-6}m^3/s]	[m/s]	[-]
■	617	0.226	1.00
○	667	0.244	0.75
◇	667	0.244	0.50
△	667	0.244	0.25
+	667	0.244	0

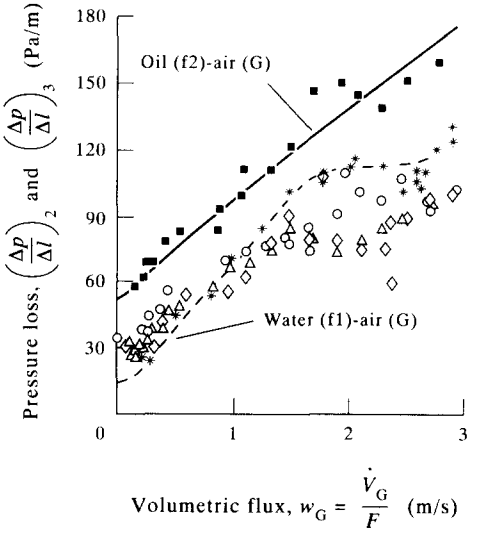

Figure 11. Measured pressure loss of two- and three-phase flows for a constant total volume flow of liquid ($\dot{V}_f = 667 \cdot 10^{-6}$ m^3/s).

4.2. *Measured Pressure Losses*

In figure 11 the measured pressure losses are presented for the two-phase gas–liquid (oil or water) flow and for the three-phase flow, as a function of the superficial flow velocity of the gas. The total volume flow rate is constant, but the oil fraction $\dot{\varepsilon}_{f2}$ is varied in steps of 25% between 0 (two-phase flow of air and water) and 100% (air and oil). The measured pressure losses of the three-phase flow can be divided into two regions, corresponding to the limiting cases of oil–air and water–air two-phase flow:

- For lower volume flow rates of the gas, the measured pressure losses in three-phase flow lie between the measured values of the respective two-phase flows. For constant values of the superficial velocity of the gas, the measured pressure losses increase, as the oil gradually replaces the water in the flow in the horizontal pipeline. The maximal value of the pressure loss is measured in the case of two-phase flow of oil and air.
- For higher volume flow rates of the gas, the measured pressure losses are lower than those for two-phase flow of water and air. In this way they are exceeding the boundaries of the region for two-phase gas–liquid flow. The measured pressure losses in this region are almost independent of the oil fraction for constant values of the superficial velocity of the liquid mixture.

The experimental results presented in figure 12 are, except for those at very low volume flow rates of the gas, obtained in the region of slug flow. The fact, that the measured pressure losses in the three-phase flow regime are lower than the values for two-phase water–air flow, can be explained by the change in the parameters of the slug: slug length, slug frequency and slug velocity for three-phase flow. The gas hold-up in the liquid slug, for example, is lower for three-phase flow compared to that for two-phase flow at the same volume flow rate.

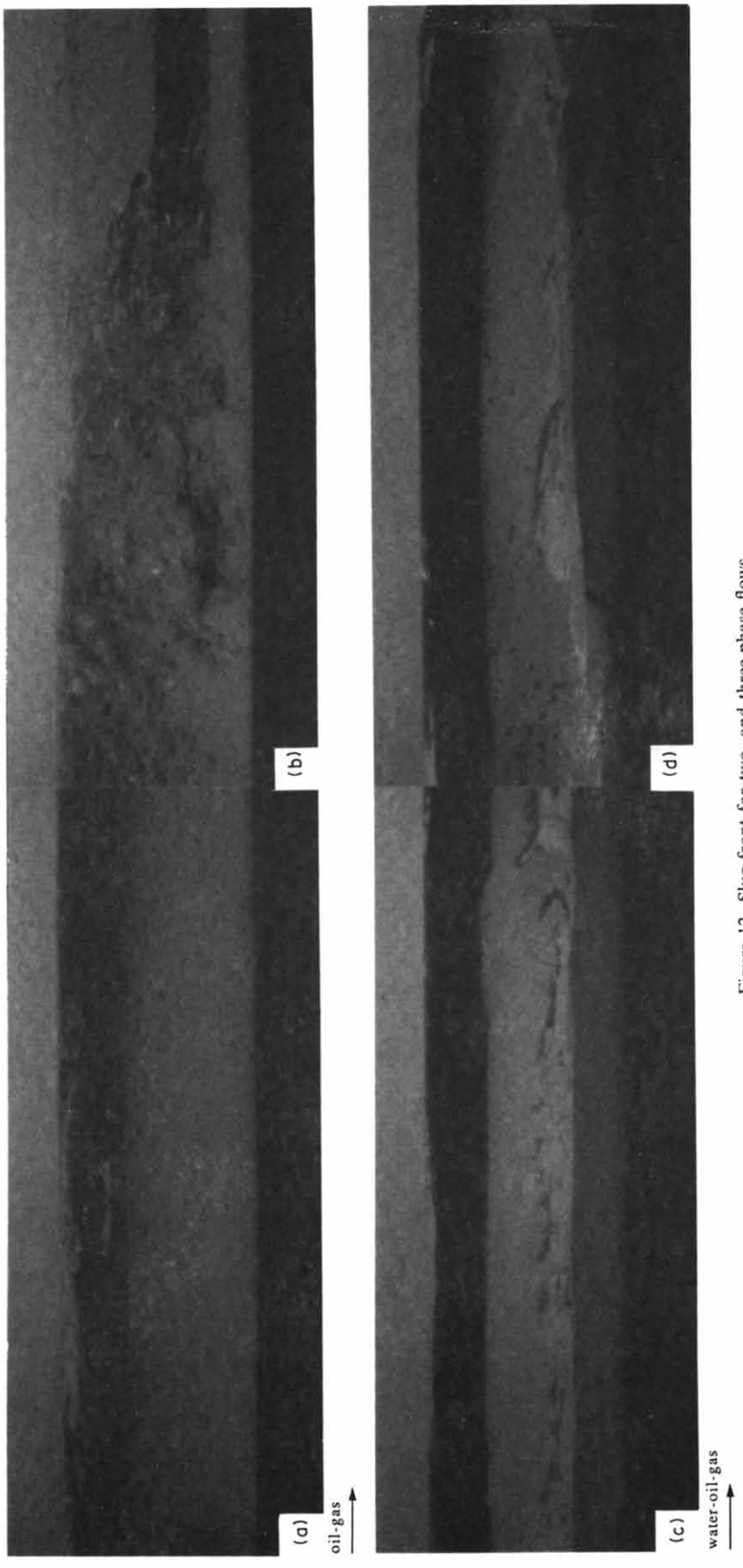

Figure 12. Slug front for two- and three-phase flows.

4.3. Slug Frequency

Experimental data of the slug frequency are presented in figure 13 as a function of the sum of the superficial velocities. Similar to the pressure loss, two characteristic regions can be observed: for low volume flow rates of the gas, the measured slug frequencies in three-phase flow are higher than the corresponding values in two-phase water–air flow, but at the same time they are lower than the values measured for two-phase oil–air flow; and for higher volume flow rates, the measured values are outside of the region defined by the two-phase flow. Independent of the oil fraction in the flow, it can be observed that, similar to two-phase gas–liquid flow, the frequency increases with increasing volume flow rate of the gas.

Calculation of the slug frequency in three-phase flow of water, oil and air is possible using the method recommended by Tronconi (1990), using the following essential assumptions:

- The slugs are formed, from stratified flow, in a similar process to that in two-phase gas–liquid flow. The oil and water flow through the tube in layers corresponding to their density. Thus, the formation of the slug is a result of the forces acting at the interface between the oil and gas. For this reason, it is assumed that the value of the coefficient C_w corresponds to the value determined for two-phase oil–air flow. For the flow of oil and air, it has been observed that every fourth liquid slug formed remains temporally stable and does not collapse. Therefore, C_w is taken to be 4.
- In order to evaluate the liquid height and mean velocity of the gas, Tronconi (1990) selected a correlation from Taitel & Dukler (1976a, b). The liquid height and the average velocity of the gas are calculated from the momentum balance for three-phase stratified flow. Therefore, it is assumed that the oil and water flow through the tube as an homogeneous mixture. In this way, the parameters required for the calculations of the slug frequency can be determined as functions of the Lockhart–Martinelli parameter, which is the ratio of the pressure losses in single-phase flows of liquid or gas:

$$\left(\frac{\Delta p}{l}\right)_2 = \Phi_{f2}^2 \left(\frac{\Delta p}{l}\right)_{f2}. \qquad [33]$$

The Lockhart–Martinelli parameter of three-phase flow is now defined as the ratio of the pressure losses in two-phase oil–water flow and single-phase gas flow. This can be written as follows:

$$X_3^2 = \frac{\Phi_{f2}^2 \left(\frac{\Delta p}{l}\right)_{f2}}{\left(\frac{\Delta p}{l}\right)_G}. \qquad [34]$$

X_3 denotes the Lockhart–Martinelli parameter of three-phase flow, and Φ_{f2}^2 denotes the correction value for a two-phase flow of oil and water. The liquid height and the superficial gas velocity can be calculated as follows:

$$X_3^2 = \frac{\left[\frac{s_G^*}{F_G^*} + \left(\frac{s_i^*}{F_f^*} + \frac{s_i^*}{F_G^*}\right)\frac{\Psi_f}{\Psi_G}\right]}{\frac{(w_f^* d_{h,f}^*)^{-n}}{(w_G^* d_{h,G}^*)^{-m}}\left(\frac{s_f^*}{F_f^*}\right)} \left(\frac{w_G^*}{w_f^*}\right)^2. \qquad [35]$$

The dimensionless parameters used in [35] are explained in table 1. In figure 14, a comparison of the calculated and measured slug frequencies is presented. For higher volume flow rates of the gas, and oil fractions above 50%, the measured and calculated frequencies are in agreement. For oil fractions of 25%, the oil layer is broken up in the inlet section. The damping influence of the oil layer on slug formation thus ceases, so that now every second slug is temporally stable. If the coefficient is $C_w = 4$, independently of the oil fraction in the flow, the mean percentage deviation between the measured and calculated values obtained using the technique described is $\pm 32\%$. In

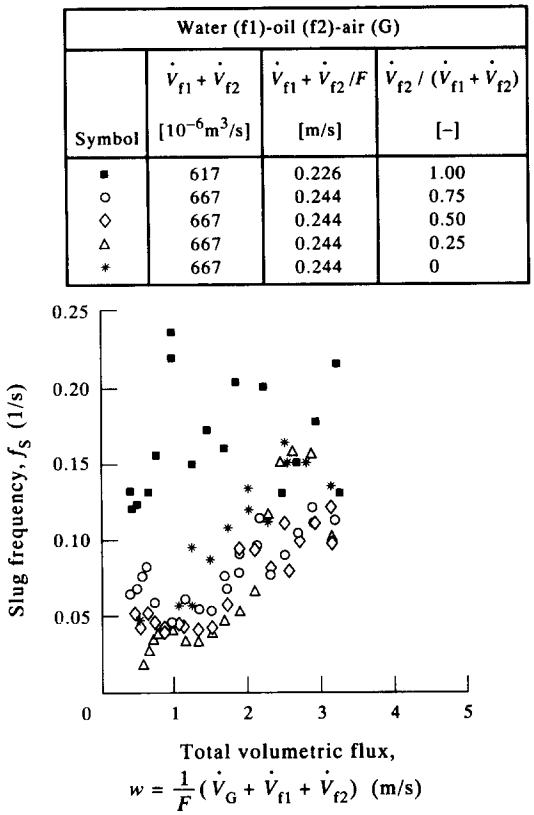

Figure 13. Slug frequency vs volumetric flux for a constant total volume flow of liquid ($\dot{V}_f = 667 \cdot 10^{-6}$ m^3/s).

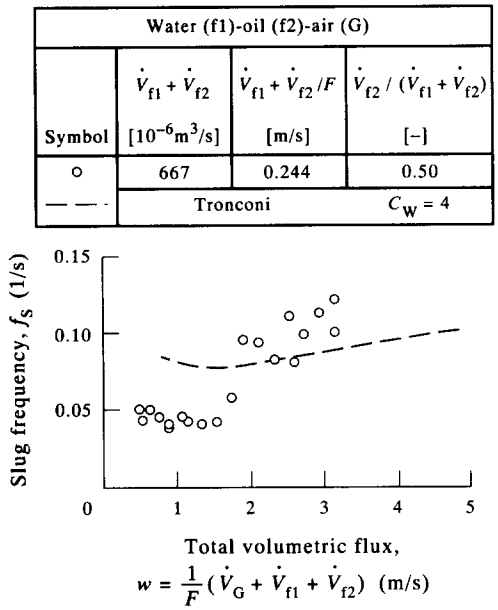

Figure 14. Comparison of the measured and predicted slug frequencies for three-phase flow.

this way, the deviation for three-phase flow is of the same magnitude as for a two-phase flow of a gas and a liquid.

4.4. Comparison of Calculated and Measured Pressure Losses

Calculation of the three-phase flow pressure loss using homogeneous or heterogeneous models is not possible. Therefore, in the following it will be explained what accuracy can be achieved when applying the procedure developed for two-phase slug flow by Dukler & Hubbard (1975) and Aziz *et al.* (1978) to three-phase flow. The slug frequency and gas hold-up in the slug body have been selected as additional input parameters for both procedures. For the calculation of the slug frequency, the method recommended by Tronconi (1990) is extended to allow for three-phase flow calculations.

In the calculation procedure for the three-phase flow pressure loss, using the methods developed by Dukler & Hubbard or Aziz *et al.*, a homogeneous oil–water flow is assumed. In figure 15, a comparison of the measured and calculated pressure losses is given. From the comparison, the following conclusions can be drawn:

- For small volumetric gas flow rates, the agreement between the measured and calculated pressure losses is good.
- The influence of the calculated frequency on the calculated pressure losses is not pronounced. In figure 15, the results of the calculations are presented, when the coefficient C_w is taken to be 2 or 4. Independently of this value, the difference between the calculated pressure losses is not significant.
- The difference between the calculated pressure losses is small when the procedure recommended by Dukler & Hubbard (1975) or that recommended by Aziz *et al.* (1978) is applied.
- For higher volumetric gas flow rates, no agreement between the calculated and measured pressure losses can be found. In this region, the measured pressure losses

are always significantly lower than the calculated ones. The maximal deviations in this region are +125%.

In order to improve the accuracy of the pressure loss calculation, the slug lengths have to be considered with known gas hold-up in the slug body as well as the slug frequency, the slug length can be calculated using both procedures. In figure 16, some of the measured slug lengths are given. For low volume flow rates of gas, the slug length in three-phase oil–water–air flow is higher than in two-phase oil–air or water–air flow. For higher volumetric gas flow rates, this influence can no longer be seen. Independent of the oil fraction in the flow, nearly constant slug lengths are measured as function of the sum of the superficial velocities.

A comparison of the measured slug lengths and the values calculated using the procedure of Aziz *et al.* is presented in figure 17. The scattering of the measured slug length is also shown in the diagram. The deviation of the slug length fluctuates, sometimes by more than 2 m around the average value. In contrast to the decrease in the measured slug length with increasing gas volume flow rates, the calculated slug lengths show a reversed behaviour. The possibility of a successful calculation of the pressure losses for low gas volume flow rates, in spite of the inaccuracies in the determination of the slug length, can be explained by the correct determination of the slug length to film length ratio. This is not the case for higher volumetric gas flow rates. The calculated slug length is too high, thus the frictional pressure loss increases, causing an increase in the total pressure loss, which is the reason for the scattering seen in figure 15.

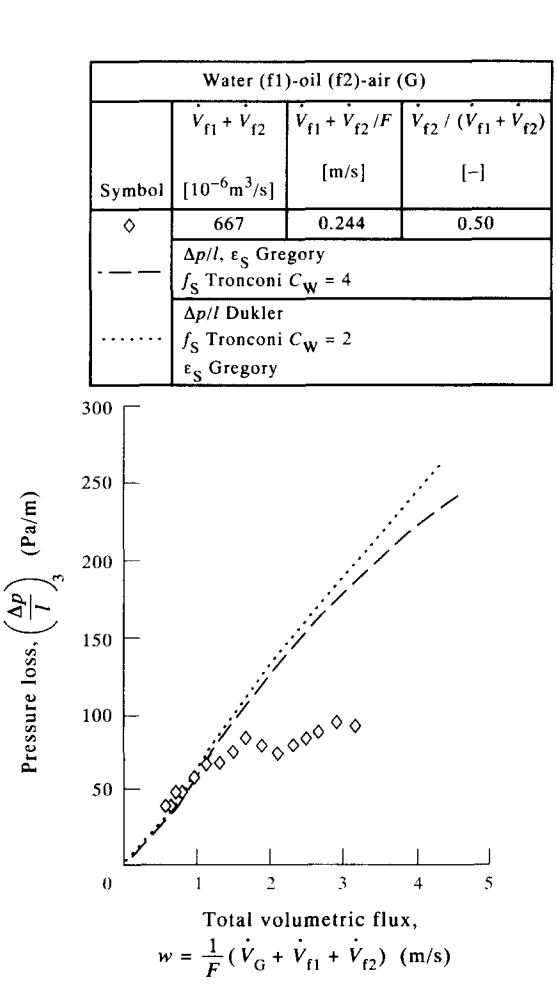

Figure 15. Comparison of the measured and predicted pressure losses for three-phase flow.

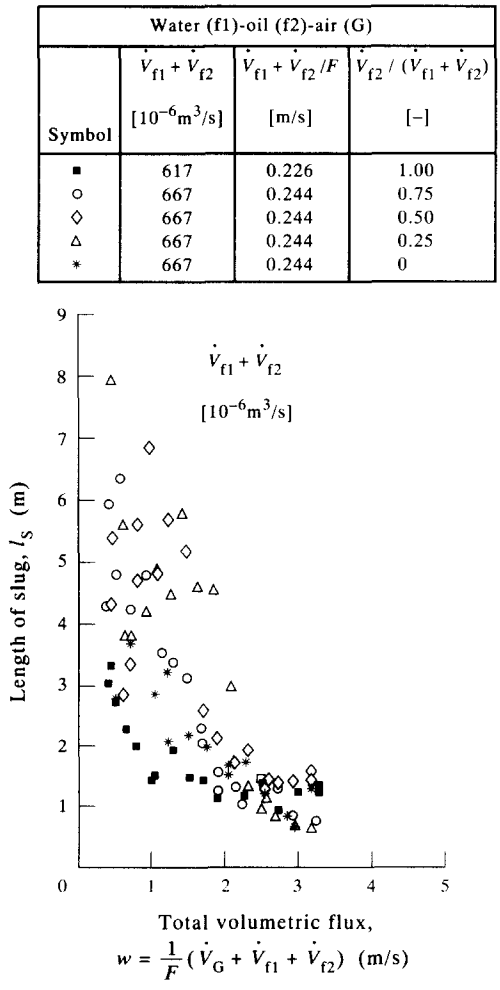

Figure 16. Measured slug length vs total volumetric flux of the three-phase mixture.

A suitable approximate solution for the evaluation of the slug length in two-phase gas–liquid flow has been recommended by Aziz *et al.* (1978). The slug length is calculated as a function of the tube diameter

$$l_s \approx 30\, d. \qquad [36]$$

Thus, for a tube diameter of 59 mm, a calculated slug length of 1.77 m results. This is, for higher volumetric gas flow rates ($w_G > 3$ m/s), in quite good agreement with the measurements.

If the measured slug length is used in the calculation of the pressure loss instead of the gas hold-up in the slug, the pressure loss in three-phase flow can be calculated with higher accuracy. This is given as an example in figure 18, for a constant volumetric liquid flow rate and a constant volumetric oil fraction. By using the above-described procedure, the measured pressure loss in three-phase flow can be reproduced with the same accuracy as in two-phase flow, for the parameter range investigated. The mean percentage deviation is $\pm 20\%$. The results can be summarized as follows:

- For low volume flow rates, the calculation of the pressure loss in three-phase flow is possible with good accuracy, for given slug frequencies. For this purpose, a procedure developed by Tronconi (1990) and extended for the analysis of three-phase flow is used. The gas hold-up in the slug body is very small at low volumetric flow rates.

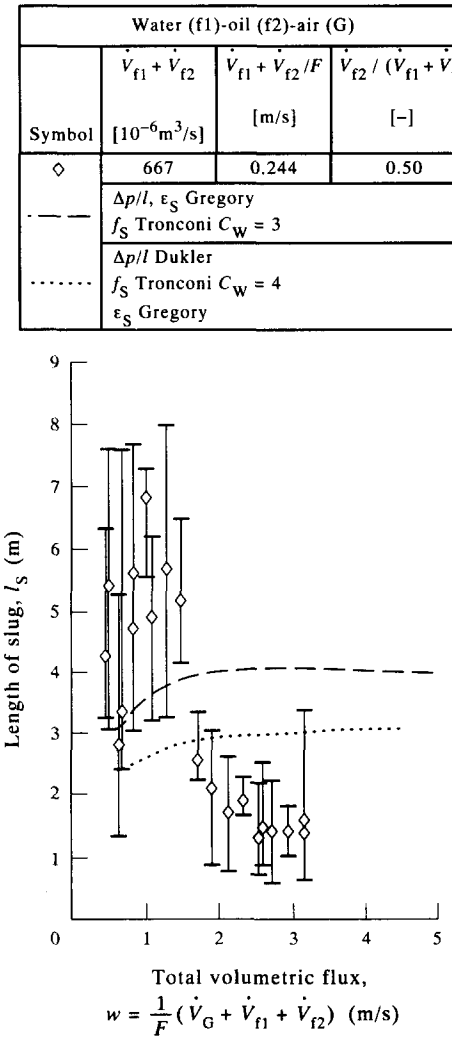

Figure 17. Comparison of the measured and predicted slug lengths.

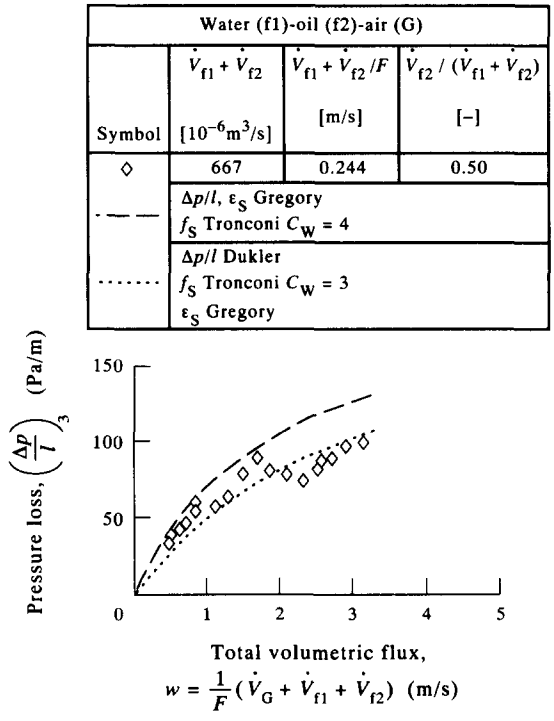

Figure 18. Predicted pressure losses with calculated slug lengths.

- This does not hold for higher volume flow rates. Either measured values of the slug length have to be known, or they have to be calculated using an approximative equation [36]. For this case, the evaluation of the pressure loss in three-phase flow is possible.

5. CONCLUSIONS

With the proposed method the prediction of the frictional pressure loss for three-phase slug flow is possible. For that purpose, the following apply:

- The slug frequencies have to be calculated for three-phase flow using new equations for the pressure loss of a flow of two immiscible liquids.
- The pressure losses have to be calculated with the known methods suggested for two-phase slug flow using homogeneous liquid properties.
- The slug length has to be estimated with the aid of a thumb rule for higher gas volume flows.

Acknowledgement—Financial support of this work by the GKSS Forschungszentrum, Geesthacht (Germany) is gratefully acknowledged.

REFERENCES

AÇIKGÖZ, M., FRANÇA, F. & LAHEY, R. T. 1992 An experimental study of three-phase flow regimes. *Int. J. Multiphase Flow* **18,** 327–336.

ARIRACHAKARAN, S., OGLESBY, K. D., MALINOWSKY, M. S., SHOHAM, O. & BRILL, J. P. 1989 An analysis of oil/water flow phenomena in horizontal pipes. In *SPE Proc. Production Operating Symp.*, Oklahoma City, OK, SPE Paper 18836.

AZIZ, K., NICHOLSON, M. K. & GREGORY, G. A. 1978 Intermittent two-phase flow in horizontal pipes—predictive models. *Can. J. Chem. Engng* **56,** 653–663.

BACKES, H. 1984 Messung und Korrelation der Grenzflächenspannung zwischen zwei flüssigen Phasen. *Fortschr. VDI Z.* **3,** 97.

BAKER, O. 1954 Designing for simultaneous flow of oil and gas. *Oil Gas J.* **53,** 185–195.

BRAUNER, N. 1991 Two-phase liquid–liquid annular flow. *Int. J. Multiphase Flow* **17,** 59–76.

CHARLES, M. 1960 The reduction of pressure gradients in oil pipelines. *Trans. Can. Inst. Min. Met.* **67,** 306–310.

CHARLES, M. & LILLELEHT, L. U. 1966 Correlation of pressure gradients for the stratified laminar–turbulent flow of two immiscible liquids. *Can. J. Chem. Engng* **44,** 47–49.

DUKLER, A. & HUBBARD, M. G. 1975 A model for gas–liquid slug flow in horizontal and near horizontal tubes. *Ind. Engng Chem. Fundam.* **14,** 337–347.

DUKLER, A., MARON, D. M. & BRAUNER, N. 1985 A physical model for predicting the minimum stable slug length. *Chem. Engng Sci.* **40,** 1379–1385.

GAZLEY, C. 1949 Interfacial shear and stability in two-phase flow. Ph.D. Thesis, Univ. of Delaware, Newark, DE.

GREGORY, G. & SCOTT, D. S. 1969 Correlation of liquid slug velocity and frequency in horizontal co-current slug flow. *AIChE Jl* **15,** 933–935.

GREGORY, G. A. & FOGARASI, M. 1985 A critical evaluation of multiphase gas–liquid pipeline calculation methods. Paper presented at the *2nd Int. Conf. on Multiphase Flow*, London.

GRESKOVICH, E. & SHRIER, A. L. 1972 Slug frequency in horizontal gas–liquid slug flow. *Ind. Engng Chem. Process Des. Dev.* **11,** 317–318.

GUZHOV, A., GRISHIN, A. D., MEDREDEV, V. F. & MEDREDEVA O. P. 1973 Emulsion formation during the flow of two immiscible liquids. *Neft. Choz.* 58–61 (in Russian).

HERM STAPELBERG, H. 1991 Die Schwallströmung von Öl, Wasser und Luft in horizontalen Rohren. Dissertation, Univ. of Hannover, Germany.

HEYWOOD, N. & RICHARDSON, J. F. 1979 Slug flow of air–water mixtures in a horizontal pipe: determination of liquid hold-up by γ-ray absorption. *Chem. Engng Sci.* **34,** 17–22.

HUBBARD, M. 1965 An analysis of horizontal gas–liquid slug flow. Ph.D. Dissertation, Univ. of Houston, TX.

KAGO, T., SARUWATARI, T., OHNO, S., MOROOKA, S. & KATO, Y. 1987 Axial mixing of liquid in horizontal two phase slug flow. *J. Chem. Engng Japan* **20,** 252–256.

KORDYBAN, E. 1961 Flow model of two-phase slug flow in horizontal tubes. *Trans. ASME Ser. D, J. Bas. Engng* **83,** 613–618.

KORDYBAN, E. 1985 Some details of developing slugs in horizontal two-phase flow. *AIChE Jl* **31,** 802–806.

KVERNOLD, O., VINDOY, V., SONTVEDT, T., SAASEN, A. & SELMER-OLSEN, S. 1984 Velocity distribution in horizontal slug flow. *Int. J. Multiphase Flow* **10,** 441–475.

LAHEY, R. T., AÇIKGÖZ, M. & FRANÇA, F. 1992 Global volumetric phase fraction in horizontal three-phase flows. *AICHE Jl* **38,** 1049–1058.

LOCKHART, R. & MARTINELLI, R. C. 1949 Proposed correlation of data for isothermal two-phase, two-component flow in pipes. *Chem. Engng Prog.* **45,** 39–48.

MISHIMA, K. & ISHII, M. 1980 Theoretical prediction of onset of horizontal slug flow. *J. Fluids Engng* **102,** 441–445.

PFENDER, C. 1986 Das strömungstechnische Verhalten von Flüssig/Flüssig-Zwei-phasenringströmungen und der Wärmeübergang an die strömenden Flüssigkeiten. *VDI-Forsch.* **634.**

TAITEL, Y. & DUKLER, A. E. 1976 A model for predicting flow regime transitions in horizontal and near-horizontal gas–liquid flow. *AIChE Jl* **22,** 47–55.

TAITEL, Y. & DUKLER, A. E. 1976 A theoretical approach to the Lockhart–Martinelli correlation for stratified flow. *Int. J. Multiphase Flow* **2,** 591–595.

TAITEL, Y. & DUKLER, A. E. 1977 A model for slug frequency during gas–liquid flow in horizontal and near-horizontal pipes. *Int. J. Multiphase Flow* **3,** 585–596.

TEK, R. 1961 Multiphase flow of water, oil and natural gas through vertical flow strings. *J. Pet. Technol.* **13,** 1029–1036.

TRONCONI, E. 1990 Prediction of slug frequency in horizontal two phase slug flow. *AIChE Jl* **36,** 701–709.

VERMEULEN, L. & RYAN, J. T. 1971 Two-phase slug flow in horizontal and inclined tubes. *Can. J. Chem. Engng* **49,** 195–201.